The Stellar Seismic Indices Data Base: Release Notes

R. Samadi

LESIA - Observatoire de Paris

Release date: 2 April 2024

Abstract

The Stellar Seismic Indices Data Base provides stellar seismic indices as well as granulation parameters extracted from red-giant stars observed with the space missions CoRoT (CNES) and Kepler (NASA). These indices were extracted using an automatic method named the MLEUP method (de Assis Peralta et al. 2016). We release here a new version of the seismic indices and granulation parameters extracted from red-giant stars observed by the Kepler and CoRoT mission. These new indices have been extracted after having identifying a problem in the pre-processing of the Kepler light-curves and by using a slightly improved version of the MLEUP method (de Assis Peralta et al. 2016). These two improvements result in higher-quality stellar indices and should significantly reduce false detections of seismic and granulation signatures. In total, seismic indices are extracted for 17,276 red-giant stars observed with Kepler. Among them, 16,557 are common wit the previous delivery of the database and 719 correspond to new stars. Finally, 1,240 Kepler stars have been removed from the previous database since they are considered as outliers with the new version of the MLEUP method. For the CoRoT light-curves, seismic indices are extracted for 3143 red-giant stars. Among them 2566 are common wit the previous delivery, 577 correspond to new stars, and 1482 stars have been removed from the database.

1   Revisited pre-processing of the Kepler light-curves

Jumps are some times seen in the light-curves. They are usually due to the occurrence of a bright pixel, which is typically generated by a particularly energetic proton impact. Because of its low orbit the CoRoT mission crossed the South Atlantic Anomaly (SAA) eight times per day. As a consequence, during the crossing of the SAA, the proton impact rate is high. Impact of particular high energetic proton can create a bright pixel in the detector leading to a sudden increase of the flux in the light curve, followed by a rather exponential decrease of variable duration. When this occurs the stellar signal is partially lost or at least strongly affected. In order to correct for the impacts of the jumps created by such events, the jump correction algorithm described in Ollivier et al. (2016) has been implemented in the SSI pipeline.

While the jump correction provides in general satisfactory results for the CoRoT light-curves, for Kepler, however, it is not necessarily useful and generate some times gaps in the light-curves, in particular for quite active stars. This is illustrated in the Fig. 1. With see in this example that the variability of the star can be misinterpreted as a jump due to the occurrence of a bright pixel. In such situation, the jump
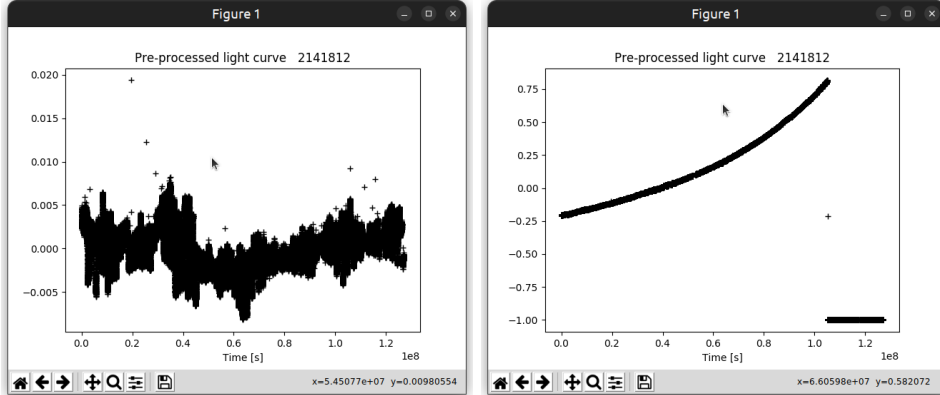
Figure 1: An example of a pre-processed Kepler light-curve without the jump correction activated (left panel) and with the jump correction activated (right panel).

correction can introduce a gap in the light-curve. This in general happen with stars showing an appreciable level of activity. Because of this, we prefer to deactivate the jump correction when pre-processing the Kepler light-curves. Actually the latter correction is not very useful because the low occurrence of bright pixels in Kepler mission.

Accordingly, we have re-processed all the long-cadence Kepler light-curves and extracted from them the stellar indices (seismic indices and granulation parameters) using the MLEUP method (in its original version de Assis Peralta et al. 2016). Comparison with the previous stellar indices does not show any significant shift of the inferred stellar indices. This is illustrated in the Fig. 2 for $\nu_{\max}$ where we compared our new estimates with the previous ones. As can been seen, the differences between the old and the new values of $\nu_{\max}$ are centred on zero while the 1-σ dispersion is equal to 0.02 μHz. The latter is negligible compared to the uncertainties associated with the derivation of $\nu_{\max}$. The same conclusions can be drawn when comparing the other stellar parameters. Our conclusion is that the gaps generated by the jump correction (which was previously activated) only weakly affect the determination of the stellar indices.

Given the large number of red-giant stars ($\sim 17,000$), it is obviously not possible to estimate by a visual inspection. In order to have a idea of the number of light-curves impacted we consider a sub-sample of $\sim 3,000$ stars for which valid seismic indices have been extracted. We consider two data sets: a sample of light-curves for which the jump correction has been turned-off (new light-curves) and a second for which the correction has been activated (old light-curves). For each star and for each data set, we compute the standard deviation $\sigma_{old/new}$. Finally, we compute the ratio $\mathcal{R} = \sigma_{old}/\sigma_{new}$. The histogram associated with the quantity $\mathcal{R}$ is displayed in Fig. 3. The median value of $\mathcal{R}$ is equal to 1.04, meaning that for half of the stars the increase of the standard deviation (resulting from the jump correction algorithm) does not exceed 4 %. The distribution is highly asymmetric. The latter is characterized by $\sigma_+ = 0.33$ and $\sigma_- = 0.04$. For 84 % of the stars, it is found that the jump correction results in an increase of the dispersion in the light-curves less than ~ 37 %. From the example shown in Fig. 1, we would have expected a larger impact, however, this is not the case because red-giant are rather quite stars (for instance the star shown in Fig. 1 is a dwarf star).
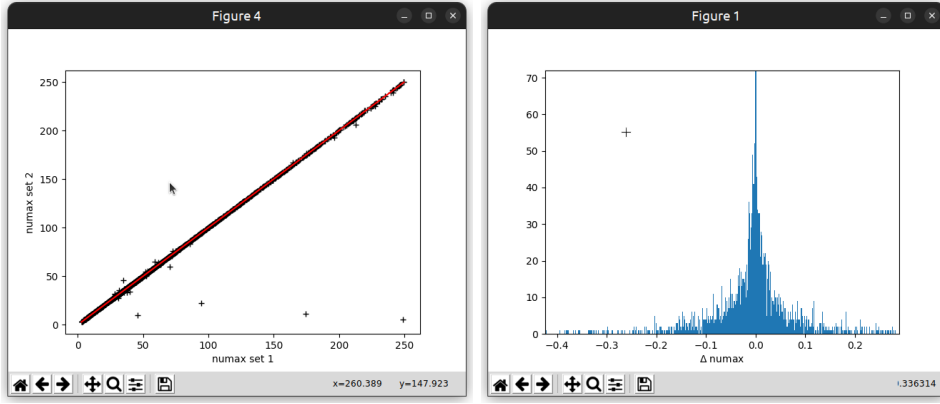
Figure 2: Left: $\nu_{\max}$ parameters extracted from light-curves with the jump correction activated (i.e. the $\nu_{\max}$ parameters corresponding to the previous release) versus $\nu_{\max}$ parameters extracted from light-curves with no jump correction (i.e. the $\nu_{\max}$ parameters corresponding to this new release). The $\nu_{\max}$ parameters are given in μHz. The red line corresponds to the one-to-one correspondence (i.e. $y = x$). Right: histogram of the difference between the two sets of $\nu_{\max}$ parameters.
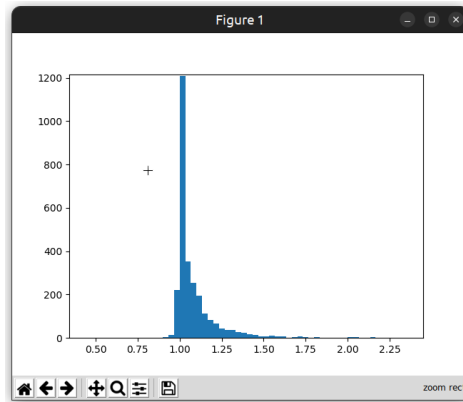
Figure 3: Histogram of the ratio $\mathcal{R} = \sigma_{old}/\sigma_{new}$ where σ_{old} (resp. σ_{new}) is the standard deviation of each given light-curves from the 'old' (resp. new) data set (see text).

3

2 Improved MLEUP method

The MLEUP method represents the envelope of the oscillation spectrum with a Gaussian function. In its original version, the width of the Gaussian function, $\delta\nu$, is a fixed parameter, which value is fixed using the following relation

$$\delta\nu_{SR} = 0.66 \, (\nu_{\max})^{0.88} \, , \tag{1}$$

where $\nu_{\max}$ is given in μHz. It is, however, possible to consider $\delta\nu$ as a free parameter without compromising the convergence of the algorithm. By considering this parameter as free, we can further improve the robustness of the extraction of seismic indices. Indeed, in some cases a spurious signal in the light-curve can be miss-interpreted as seismic signal. For instance a single peak in the spectrum can be miss-interpreted as the presence of a power excess. However, in such case the width $\delta\nu$ generally converges toward a rather low value, located far outside the range of physically admissible values. Accordingly, we can remove a wrong identification of a seismic signal when the fitted value of $\delta\nu$ is far from the value given by the scaling relation of Eq. 1. Accordingly, we retain only the stars for which

$$\frac{1}{5} \, \delta\nu_{SR} < \delta\nu < 5 \, \delta\nu_{SR} \, , \tag{2}$$

where $\delta\nu_{SR}$ is given by Eq. 1.

Furthermore, the MLEUP method remove outliers in the seismic indices by keeping only the stars for which the large separation $\Delta\nu$ and the envelope height H_{env} verify the following condition:

$$\left(\frac{\Delta\nu - \Delta\nu^{\mathrm{SR}}}{\alpha_{\pm}\Delta\nu^{\mathrm{SR}}}\right)^2 + \left(\frac{H_{\mathrm{env}} - H_{\mathrm{env}}^{\mathrm{SR}}}{\beta_{\pm}H_{\mathrm{env}}^{\mathrm{SR}}}\right)^2 \leqslant 1 \, , \tag{3}$$

with $\alpha_+ = \alpha_- = 0.30$, $\beta_+ = 3$ and $\beta_- = 1$. $\beta_+ \neq \beta_-$ because the distribution of results for the parameters H_{env} is asymmetric. X^{SR} is the value of the parameter X corresponding to the scaling relation de Assis Peralta et al. (for details see 2016). However, we notice that the condition imposed on H_{env} is too restrictive when $\delta\nu$ is adjusted and found that adopting $\beta_+ = 15$ and $\beta_- = 5$ is more optimal.

3 Quick look of the new stellar indices

4 Kepler stars

After having re-processed all the Kepler light-curves without activating the jump correction we applied the MLEUP on all of them. From a total of 203,598 light-curves, valid seismic indices are detected for 17,276 stars and valid granulation parameters for 13,701 stars.

The seismic indices found with this new analysis (the current release) are displayed in Fig. 4. For the granulation parameters, the results are displayed in Fig. 5.

5 Comparison with the previous stellar indices

The Fig. 6 shows a comparison of the new values of $\nu_{\max}$ with the old ones. We analysed the difference between the new and the old values of $\nu_{\max}$. We see a systematic shift of about $+1$ νHz, which is significant if we compare it to the dispersion ($\sim 1 \, \mu$Hz). This shift increases with $\nu_{\max}$: as $\nu_{\max}$ increases, the new values of $\nu_{\max}$ are progressively larger than the old values. The Fig. 7 shows the same
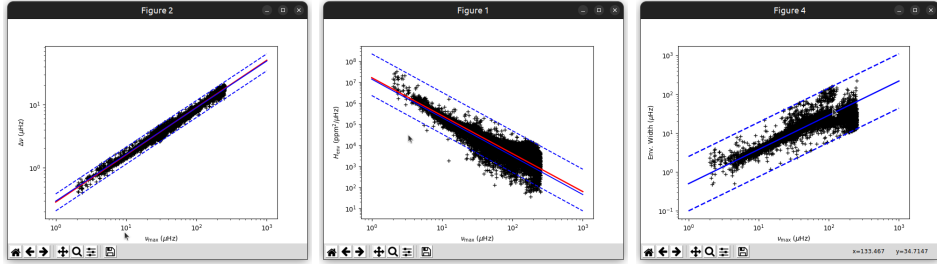
Figure 4: The new seismic indices (this release). Left: $\nu_{\max}$ as a function of $\Delta\nu$. Middle: height of the envelop, H_{env}, as a function of $\nu_{\max}$. Right: the width of the envelop, $\delta\nu$, as a function of $\nu_{\max}$.
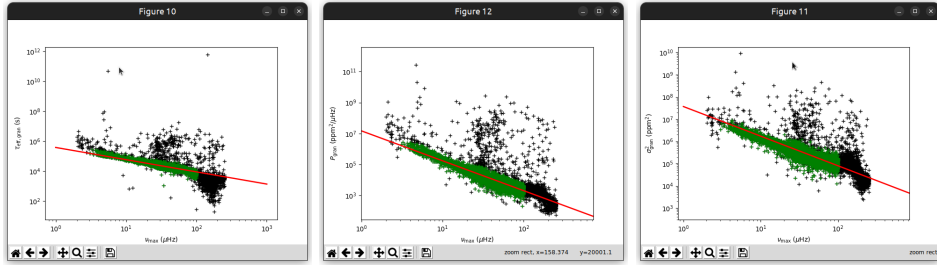

Figure 5: The new granulation parameters as a function of $\nu_{\max}$. Left: the e-folding time, τ_e. Middle: the height of the granulation component, P_g. Right: σ_g^2, where σ_g is the amplitude of the granulation component. The green symbols correspond to the granulation parameters that are considered valid (see de Assis Peralta et al. 2016).
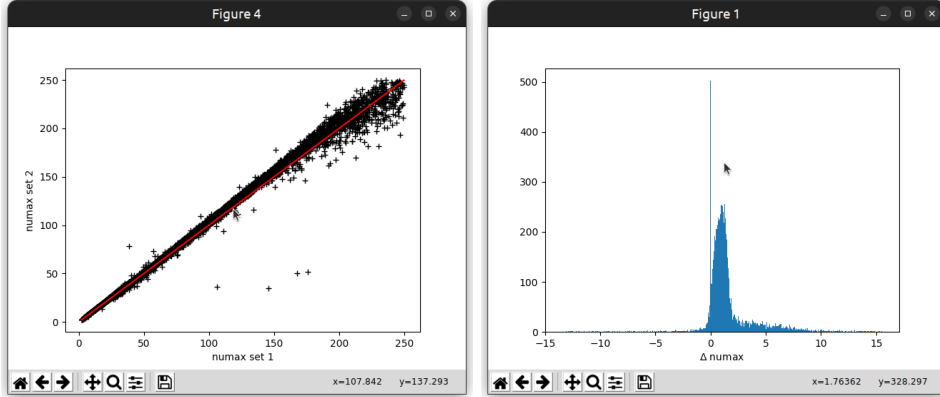
Figure 6: Left: new values of ν_{max} versus olde ones. The ν_{max} parameters are given in μHz. The red line corresponds to the one-to-one correspondence (i.e. $y = x$). Right: histogram of the difference between the two sets of ν_{max} parameters.
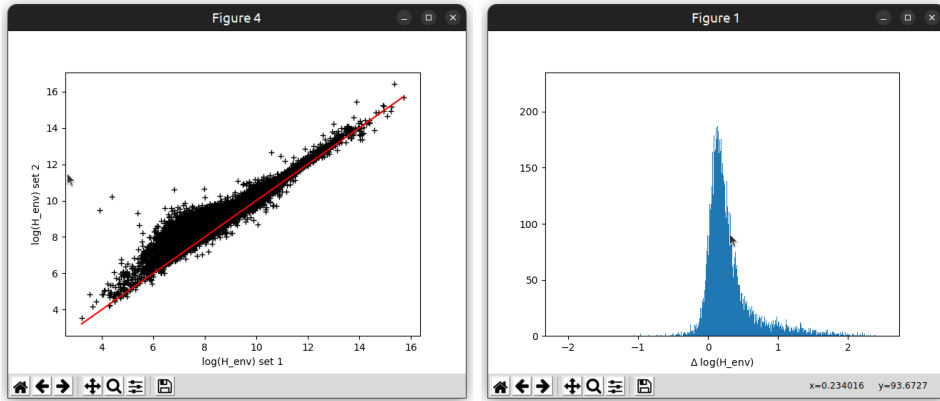

Figure 7: As in Fig. 6 for $\log H_{\mathrm{env}}$, where H_{env} is the height of the envelope.

for H_{env}, the height of the envelope. As for ν_{max}, $\log H_{\mathrm{env}}$ is subsect to a systematic shift of 0.2 whereas the 1-σ dispersion is equal to 0.25. Accordingly, the systematic shift is significant. For $\Delta\nu$ (see Fig. 8), the systematic shift is about - 1 nHz and the dispersion is asymmetric and equal to $\sigma_+ \simeq 1$ nHz and $\sigma_+ \simeq -2.3$ nHz. Finally, for the stellar parameters the distributions are all centred nearly on zero (see Fig. 9-10) and the systematic shifts are negligible.

6   CoRoT

We first note that the CoRoT light-curves are not concerned by the problem of the jump correction mentioned in Sect 1. Indeed, the pre-processing of the CoRoT has been done by turning off the jump correction since the official CoRoT pipeline operates an efficient jump correction (see Ollivier et al. 2016).

The CoRoT light-curves have been re-processed with the new version of MLE-UP. From a total of 117,774 light-curves, valid seismic indices are detected for 3143 stars and valid granulation parameters for 1035 stars. For all stellar indices, comparison with the new and previous indices shows no significant differences.
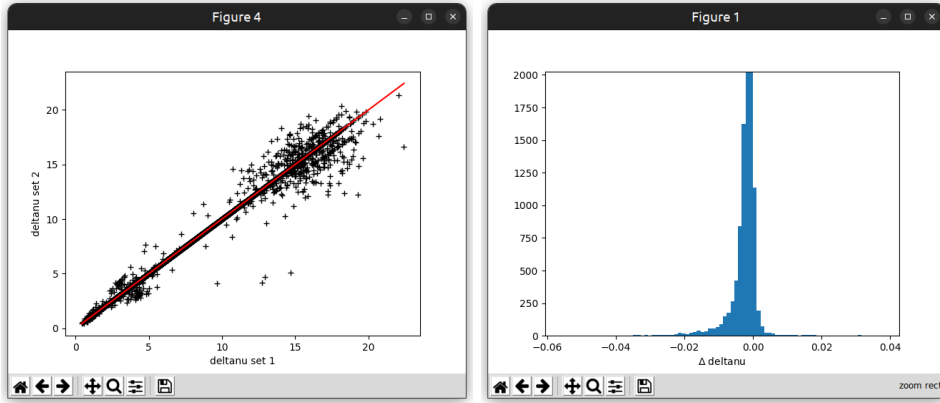
Acknowledgements

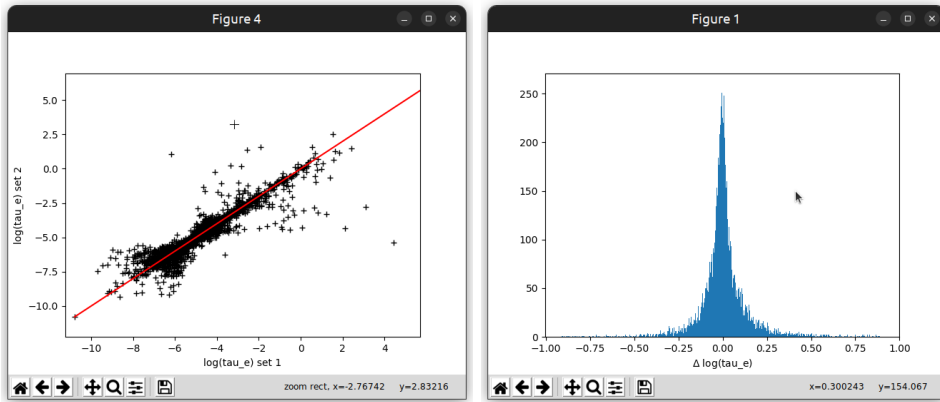Figure 8: As in Fig. 6 for the large separation $\Delta\nu$.

Figure 9: As in Fig. 6 for $\log \tau_e$, where τ_e is "e-folding" time effective associated with the granulation signal.
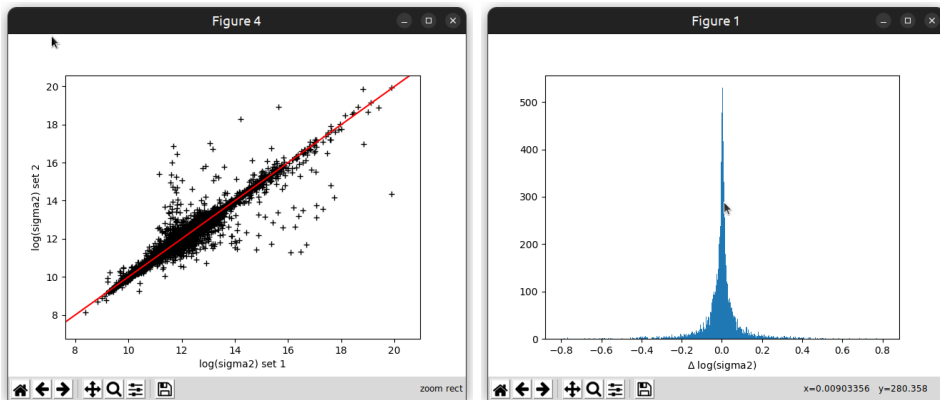

Figure 10: As in Fig. 6 for $\log \sigma_g^2$, where σ_g is amplitude of the granulation signal.

References

de Assis Peralta, R. A., Samadi, R., & Michel, E. 2016, MNRAS, submitted

Ollivier, M., Deru, A., Chaintreuil, S., et al. 2016, II.2 Description of processes and corrections from observation to delivery, ed. CoRot Team, 41